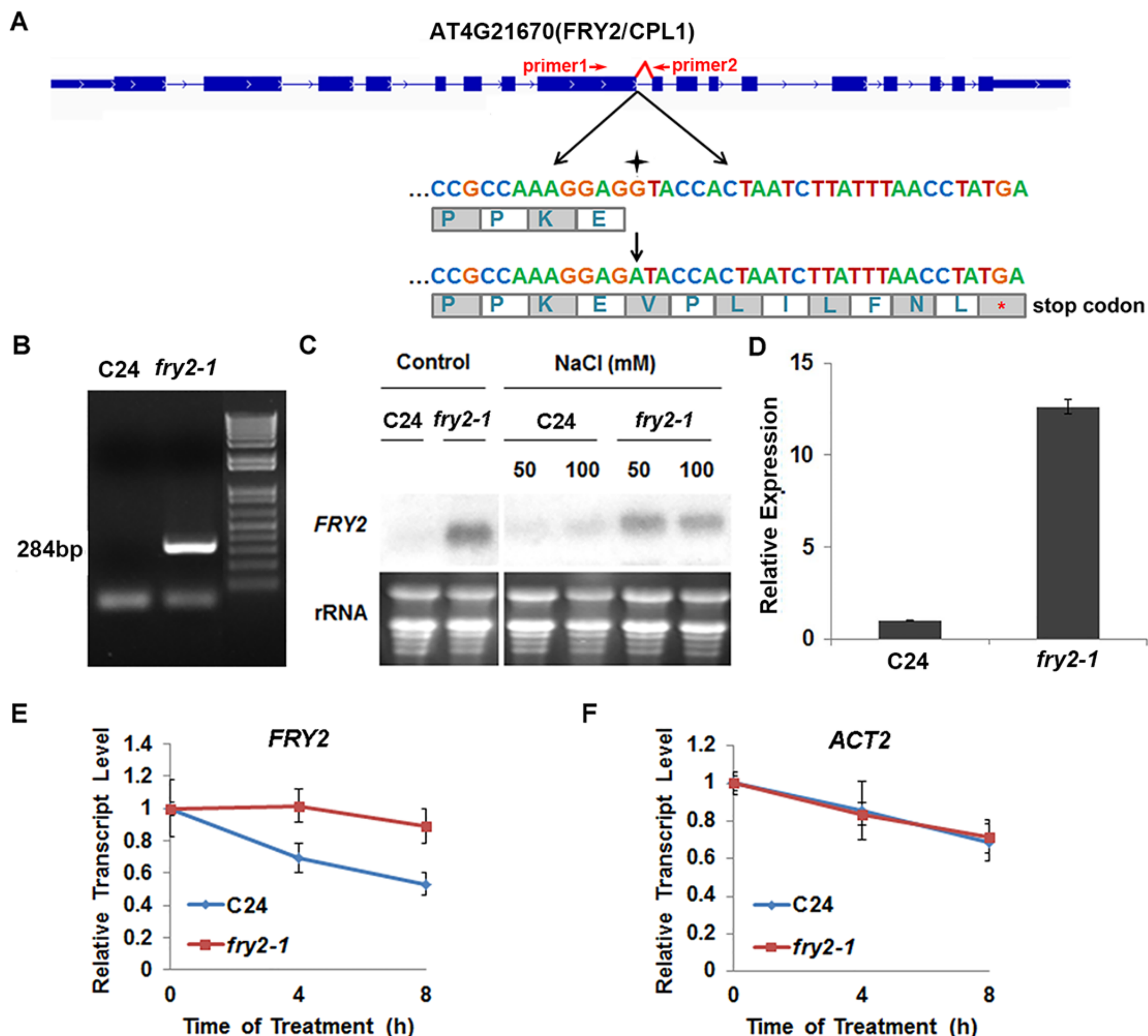

Supplemental Figure 1 Accumulation of PTC-containing *FRY2* transcripts in the *fry2-1* mutant. (A) Exon-intron structure of the *FRY2* gene was given at the top of the panel. The black star symbol indicates the mutation of *fry2-1*. The intron retention introduces a premature stop codon (marked by *). (B) Two variants of *FRY2* transcripts were validated by RT-PCR using intron-flanking primers (marked by red arrows on the gene structure). The two bands in *fry2-1* represent transcripts with (upper) and without (lower) the intron, respectively. (C) RNA blotting examination of the *FRY2* expression levels in the wild type and the mutant. Ribosomal RNA was used as a loading control. (D) The expression levels of *FRY2* were detected by quantitative RT-PCR in the wild type and mutant. (E) PTC-containing *FRY2* transcripts are more stable in *fry2-1*. 12-day-old seedlings of C24 and *fry2-1* were subject to 200 μM Triptolide (TPL) treatment for 0, 4 and 8 hours and total RNAs were extracted. Quantitative real-time RT-PCR was performed to determine the transcriptional levels. *ACT2* was used as a control (F). Error bars represent standard deviations (n=3).

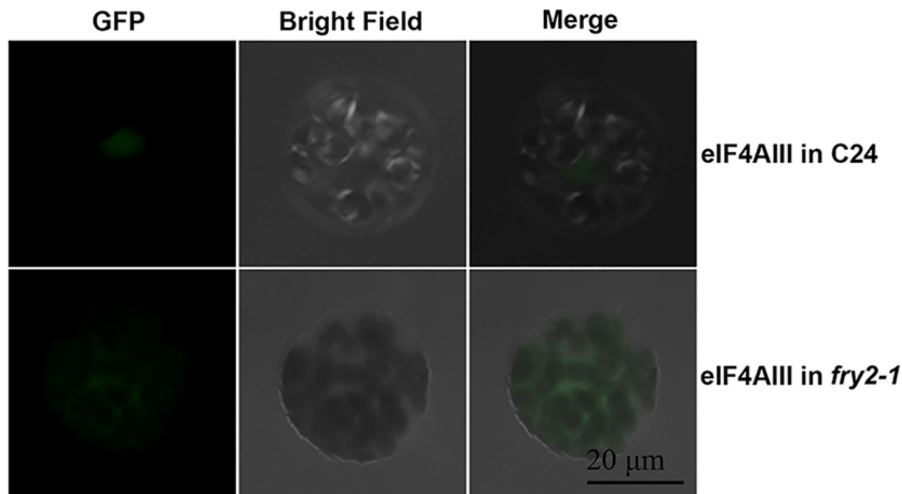

Supplemental Figure 2 Mis-localization of eIF4AIII in *fry2-1*. GFP-fused eIF4AIII construct with the eIF4AIII native promoter was transformed into protoplasts of C24 and *fry2-1*. Images were taken using a confocal microscope. Left panels, GFP signals; middle panels, bright field images; right panels, merged images. Scale bars = 20 μm.

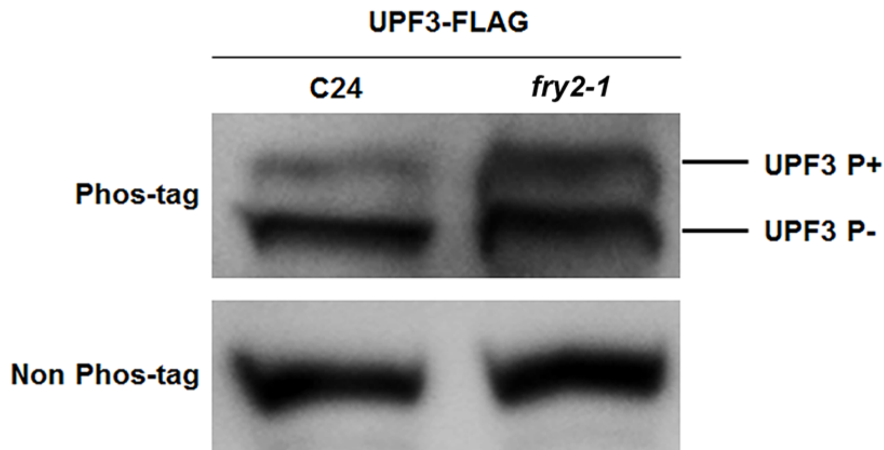

Supplemental Figure 3 Phosphorylation level of UPF3 could be regulated by FRY2 in vivo. Total protein extracts from wild type C24 and *fry2-1* seedlings expressing FLAG-tagged UPF3 were subjected to SDS-PAGE containing Phos-tag. UPF3 signals were detected by anti-FLAG M2 antibody. Upper and lower bands could be phosphorylated and unphosphorylated UPF3, respectively. Non-phos-tag gel was used as control.

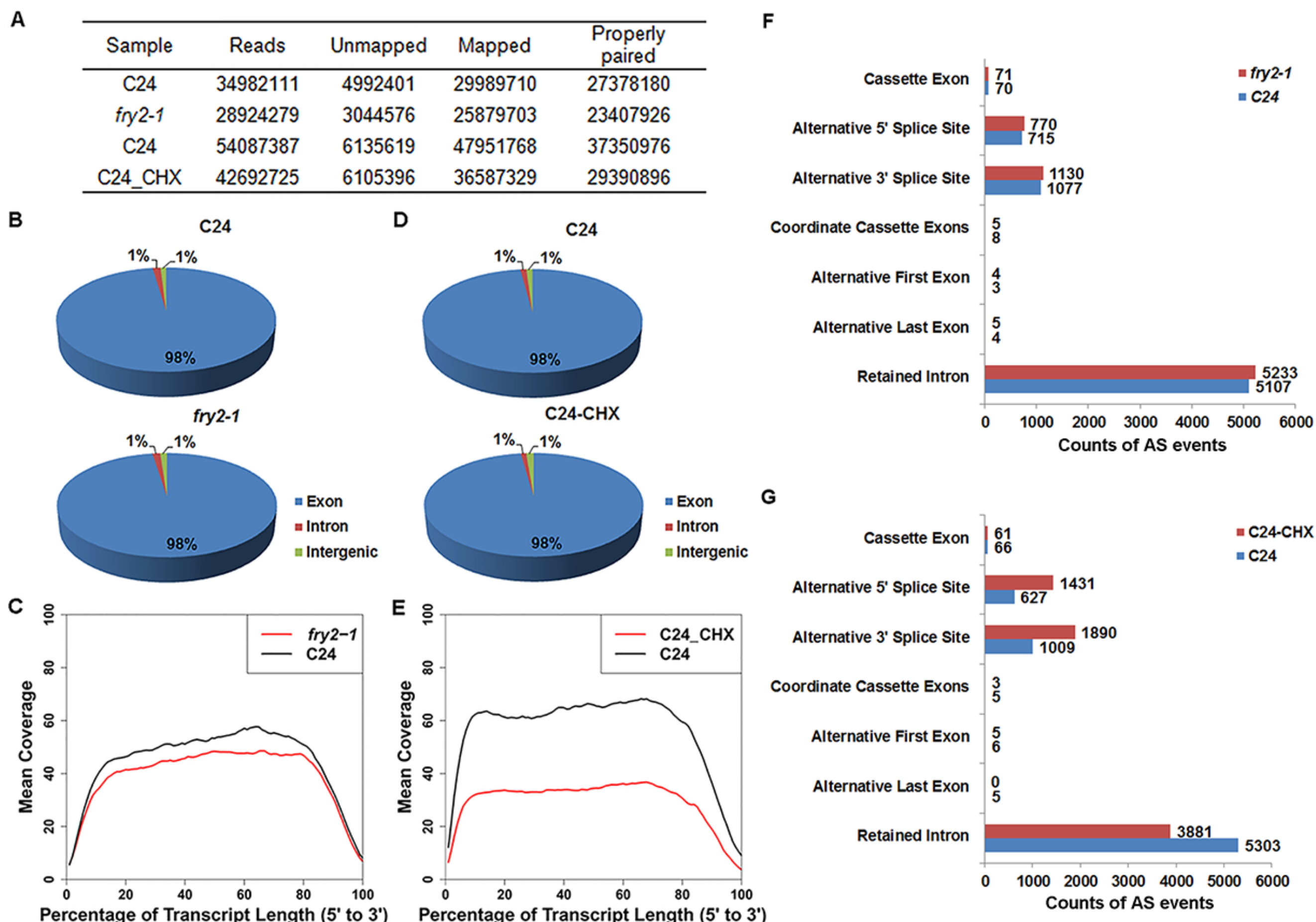

Sample	Reads	Unmapped	Mapped	Properly paired
C24	34982111	4992401	29989710	27378180
fry2-1	28924279	3044576	25879703	23407926
C24	54087387	6135619	47951768	37350976
C24_CHX	42692725	6105396	36587329	29390896

Supplemental Figure 4 Quality analyses of RNA-seq data from *fry2-1* mutant and CHX-treated wild type (C24) and identification of AS events. (A) Mapping results of RNA-seq reads. (B) Distribution of the RNA-seq reads in the *fry2-1* mutant along annotated Arabidopsis genomic features. Among reads that unambiguously match the Arabidopsis genome, more than 90% of reads match to annotated exons. (C) Distribution of RNA-seq read coverage in the *fry2-1* mutant was plotted along the length of the transcriptional unit. *x*-axis indicates the relative length of transcripts, and *y*-axis shows the median depth of coverage. (D) Distribution of the RNA-seq reads in CHX-treated wild type (C24) along annotated Arabidopsis genomic features. (E) Distribution of RNA-seq read coverage in CHX-treated wild type (C24) was plotted along the length of the transcriptional unit. (F-G) Identification of AS events. Each type of AS events was counted in the *fry2-1* mutant (F), the CHX-treated wild-type plants (G) and the control plants.

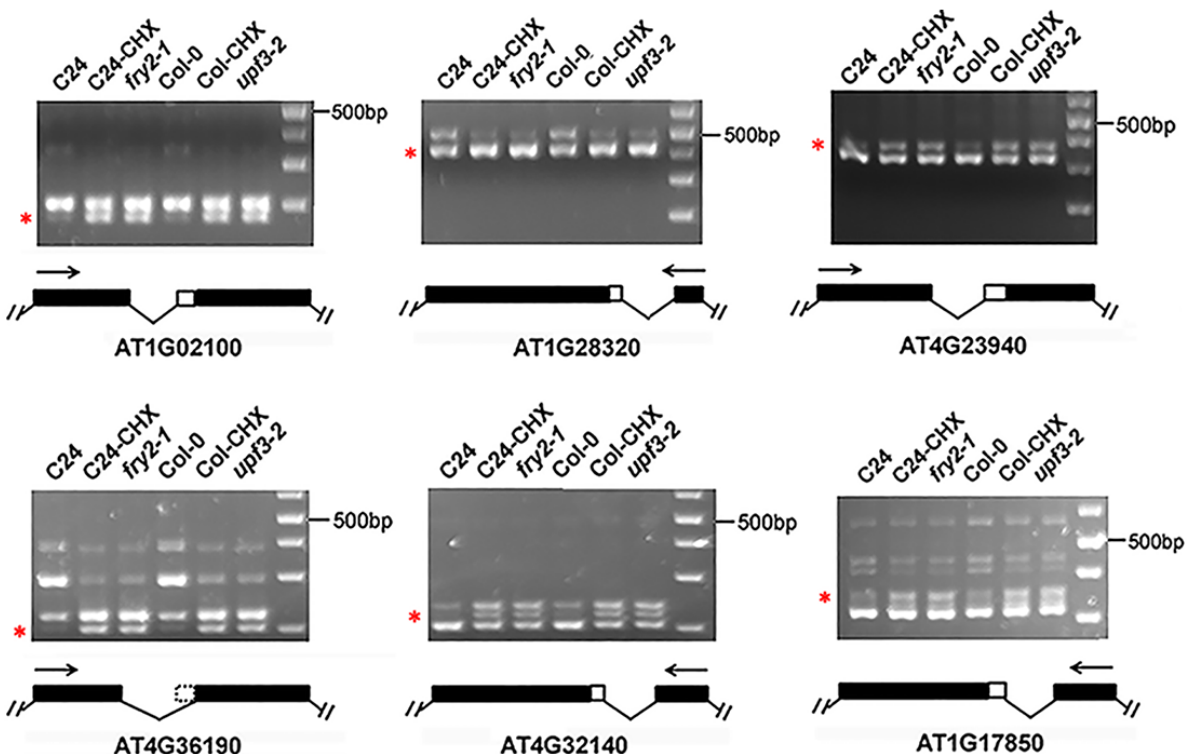

Supplemental Figure 5 Six representative AS events validated by RT-PCR and depicted by partial gene model. The bands marked by asterisks (*) represented the alternative-splice isoforms, which were more obviously detected in *fry2-1*, CHX-treated wild type (C24 or Col-0), and the *upf3-2* mutant plants, than in the control plants. At the bottom, the gene models with boxes and lines (representing exons and introns, respectively) for the AS transcripts are shown. Black boxes show coding regions (according to the representative gene model annotated at TAIR10), and white boxes indicate the alternatively spliced region. Arrows represent the direction of gene transcription.

A

Sample	Reads	Unmapped	Mapped	Uniquely mapped
Col-0	21692737	703255	20989482	20207957
upf3-1	32210315	373631	31836684	30429558

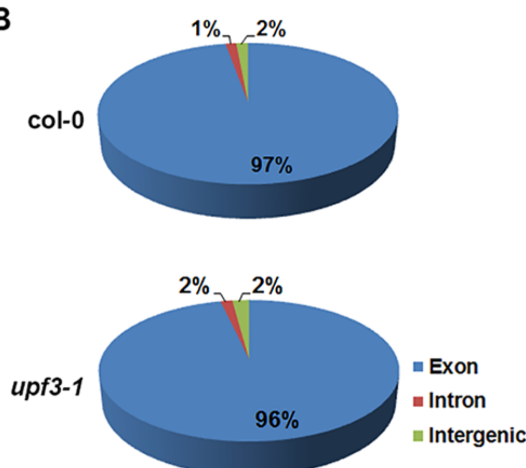

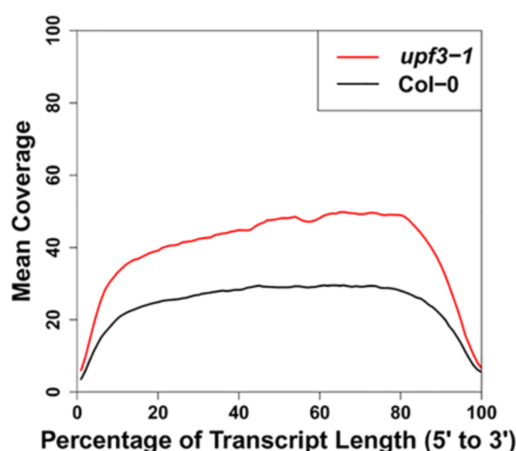

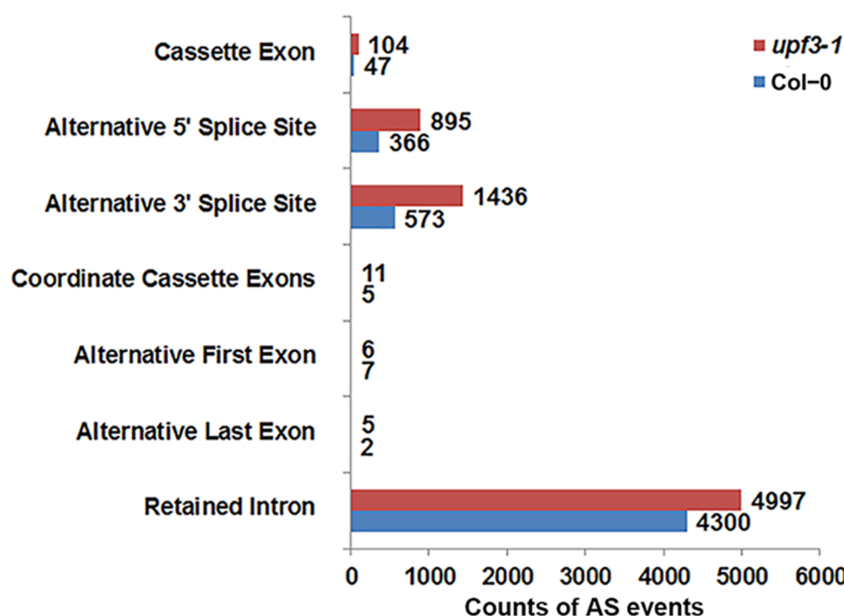

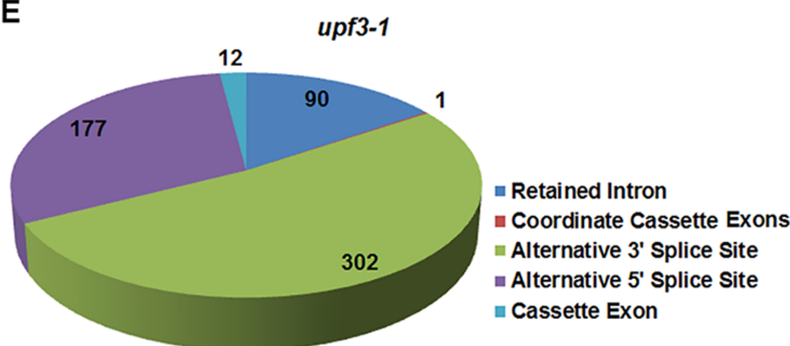

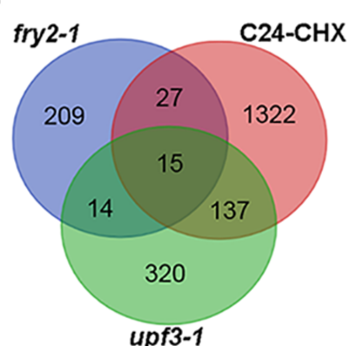

Supplemental Figure 6 Quality analyses of the RNA-seq data for *upf3-1* and identification and comparison of AS events. (A) Mapping results of RNA-seq reads. (B) Distribution of the RNA-seq reads in the wild type Col-0 and *upf3-1* mutant along annotated Arabidopsis genomic features. (C) Distribution of RNA-seq read coverage was plotted along the length of the transcriptional unit. *x*-axis indicates the relative length of transcripts, and *y*-axis shows the median depth of coverage. (D) Identification of AS events. Each type of AS events was counted in Col-0 and *upf3-1* mutant. (E) Identification and annotation of AS events that were over-represented in the *upf3-1* mutant compared with those in Col-0. (F) Comparison of AS events among *fry2-1*, CHX-treated C24 and *upf3-1*.

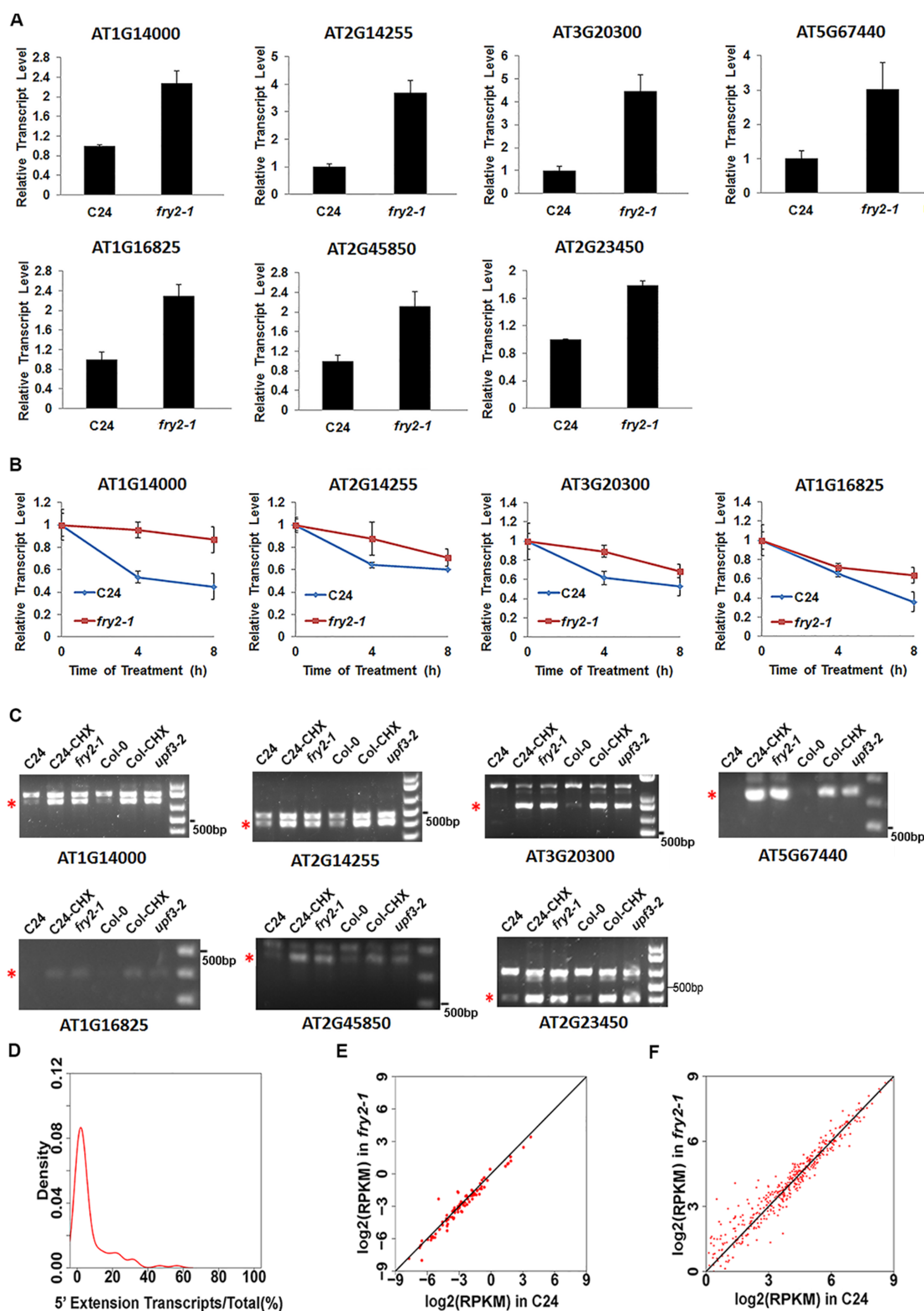

Supplemental Figure 7 Accumulation of 5'-extended mRNAs in the *fry2-1* mutant. (A) The expression levels of seven 5'-extended mRNAs in C24 and *fry2-1* were measured by quantitative RT-PCR. (B) The 5'-extended mRNAs are more stable in *fry2-1*. 12-day-old seedlings of C24 and *fry2-1* were subject to 200 μM Triptolide (TPL) treatment for 0, 4 and 8 h and total RNAs were extracted. Quantitative real-time RT-PCR was performed to determine the transcriptional levels. *ACT2* was used as a control. Error bars represent standard deviations (n=3). (C) The level of these 5'-extended mRNAs marked by asterisks (*) in the gel picture was higher in *fry2-1*, CHX-treated wild type (C24 or Col-0), and the *upf3-2* mutant plants than in the control plants. (D) Distribution of the proportion of 5'-extended mRNAs to the total transcripts for each affected gene in the *fry2* mutant. The percentage is calculated by dividing the RPKM value of the 5'-extended region by the RPKM value of the affected gene. (E) Comparison of expression levels (RPKM) of the genes with 5'-extended mRNAs between the wild type and the *fry2-1* mutant. RPKM, reads per kilobase per million mapped reads. (F) Expression levels (RPKM) of 500 random-selected genes (as a control) were compared between the wild type and the *fry2-1* mutant.